SOLUTION CONFORMATION OF THE DISACCHARIDE OF AVERMECTIN B_{1a} EXAMINED BY NMR SPECTROSCOPY AND NUCLEAR OVERHAUSER ENHANCEMENT RESTRAINED HARD-SPHERE EXO-ANOMERIC EFFECT CALCULATION

ANDRÁS NESZMÉLYI, DAISY MACHYTKA, ANDREA KMETY, PÉTER SÁNDOR and GABOR LUKACS†

Central Research Institute for Chemistry, Hungarian Academy of Sciences, H-1025 Budapest, Pusztaszeri ut 59, Hungary
†Institut de Chimie des Substances Naturelles du C.N.R.S., F-91190 Gif-sur-Yvette, France

(Received for publication January 31, 1989)

The solution conformation of the disaccharide of avermectin B_{1a} was examined by combining NMR data with theoretical conformational energy calculations.

Carbon and proton resonances were assigned unambiguously using high-field, high-resolution 2D NMR correlation spectroscopy. $^3J_{HH}$ coupling constants were determined at 600 MHz.

The minimum-energy conformation was attained through an extended hard-sphere exo-anomeric effect (HSEA) approach. The HSEA conformation was refined by considering the experimental nuclear Overhauser enhancement contacts. The resulting three-dimensional structure was confirmed by comparing its glycosidic dihedral angles to those calculated from experimental $^3J_{COCH}$ coupling constants.

Differences has been found in the glycosidic dihedral angles between the solution conformation and the X-ray structure.

Recent results of the application of the hard-sphere exo-anomeric effect (HSEA) method[1,2] to the solution conformation problem of glycoconjugates[3~5] prompted us to study its potential in the case of a macrolide antibiotic of considerable biological interest[6] made up of a macrocycle and a disaccharide unit. The importance of the disaccharide is demonstrated by the fact that its loss diminishes the anthelmintic activity to about 5% of that of the parent compound. Although the chemical structure of avermectin B_{1a} is known, its dynamics and solution conformation has not been investigated.

Results and Discussion

For the conformational analysis of the antibiotic it was necessary to have unambiguous assignments of its ^1H and ^{13}C NMR spectra, with special emphasis on those atoms which are important for determining the conformation. ^{13}C NMR chemical shifts were already published[6], but unambiguous ^1H NMR parameters for avermectin B_{1a} are not available in the literature. The present assignment is complete and is based on ^1H-^1H and ^1H-^{13}C chemical shift correlation experiments. Coupling constants were derived from one-dimensional spectra taken at 600 MHz and checked by spin simulation. Table 1 contains all NMR chemical shifts and coupling constants determined in this work.

Comparing our ^{13}C data to those found in the literature[6] additional information was obtained: The resonances of C-2′ and C-2″ could be resolved and assigned, and also evidence was found for the reversal of the original assignments[6] of C-6′ and C-6″. The correct assignment of the two OCH_3 signals (3′-OCH_3 and 3″-OCH_3) was possible only by using T_1 relaxation data.

Table 1. Chemical shifts (ppm) and coupling constants (Hz) of avermectin B_{1a} (determined at H_0= 9.395 T).

Atom	δ (^{1}H)	$^3J_{HH}$	$^nJ_{HH}$	δ (^{13}C)	$^1J_{CH}$	$^3J_{CH}$
1				173.6 s		$J_{C\text{-}1,19\text{-}H}$=9.0
2	3.284 qdd	2.2	2.3 (4a)	45.7 d		
3	5.408 ddd	—	1.6 (4a)	118.2 d		
			0.8 (5)			
4	—	—		137.8 s		
4a	1.859 ddd	—	0.8 (5)	19.9 q		
5	4.277 dddq	6.24		67.7 d	142.7	
6	3.953 d	—		79.2 d	146.7	
7	—	—		80.3 d		
7-OH	3.98 br	—		—		
8	—	—		139.5 s		
$8a_\alpha$	4.681 ddd	2.55		68.3 t	149.0	$J_{C\text{-}8a,9\text{-}H}$=8.7
		−14.29 ($8a_\beta$)				
$8a_\beta$	4.655 ddd	2.42				
9	5.86 dd	10.6	*ca.* 1 (11)	120.3 d		
10	5.73 dddd	−14.6	*ca.* 1 (12)	124.7 d		$J_{C\text{-}10,12\text{-}H}$=5.5
11	5.74 dddd	9	*ca.* 2 (13)	138.0 d		
12	2.510 dqd	*ca.* 2.5 (13)		39.7 d		
		7.0 (12a)				
12a	1.153 d	—		20.2 q		
13	3.924 br q	—	*ca.* 2 (15)	81.9 d	144.3	$J_{C\text{-}13,1'\text{-}H}$=3.1
14	—	—		135.1 s		
14a	1.480 d	—		15.1 q		
15	4.978 ddqd	10.7 (16_{ax})		118.0 d		
		ca. 3 (16_{eq})				
16_{ax}	2.29 br	−12.6 (16_{eq})		34.2 t		
		10.3 (17)				
16_{eq}	2.26 br	5.1				
17	3.864 dddd	11.7 (18_{ax})		68.3 d		
		2.3 (18_{eq})				
18_{ax}	0.86 dt	11.7 (19)		36.5 t		
		−12.6 (18_{eq})				
18_{eq}	1.767 dddd	4.7 (19)	1.98 (20_{eq})			
19	5.388 tt	11.6 (20_{ax})		68.3 d		
		4.8 (20_{eq})				
20_{ax}	1.472 t	−12.0 (20_{eq})				
20_{eq}	2.002 ddd			40.5 t		
21				95.8 s		
22	5.749 dd	9.86	1.81 (24)	136.3 d		
23	5.536 dd	2.62		127.7 d	160.7	
24	2.253 dqdd	9.9 (25)		30.5 d		
		7.2 (24a)				
24a	0.902 d			16.4 q		
25	3.468 dd	1.8		74.9 d	142.0	
26	1.586 dqd	6.8 (26a)		35.1 d		
		<0.5 (27_α)				
		13.9 (27_β)				
26a	0.906 d			13.0 q		
27_α	1.538 dq	7.4 (28)		27.5 t		
		−13.3 (27_β)				
27_β	1.466 ddq	7.4 (28)				
28	0.924 t			12.0 q		

Table 1. (Continued)

Atom	δ (^{1}H)	$^3J_{HH}$	$^nJ_{HH}$	δ (^{13}C)	$^1J_{CH}$	$^3J_{CH}$
1′	4.758 ddd	4.1 (2′$_{ax}$) 1.51 (2′$_{eq}$)		94.9 d	167.0	$J_{C\text{-}1',13\text{-}H}$=4.1
2′$_{eq}$	2.208 ddd	4.9 (3′) −13.0 (2′$_{ax}$)		34.4 t		
2′$_{ax}$	1.564 ddd	11.5 (3′)				
3′	3.609 ddd	8.6 (4′)		79.3 d		$J_{C\text{-}3',1'\text{-}H}$=6.2
3′-OCH$_3$	3.423 s			56.5 q		
4′	3.228 dd	9.38 (5′)		80.3 d	140.4	$J_{C\text{-}4',1''\text{-}H}$=3.7
5′	3.820 dq (d)	6.27 (6′)		67.2 d		$J_{C\text{-}5',1'\text{-}H}$=7.5
6′	1.241 d			18.4 q		
1″	5.379 ddd	4.0 (2″$_{ax}$) 1.38 (2″$_{eq}$)		98.4 d	170.5	$J_{C\text{-}1'',4'\text{-}H}$=5.2
2″$_{eq}$	2.320 ddd	4.8 (3″) −12.8 (2″$_{ax}$)		34.2 t		
2″$_{ax}$	1.511 ddd	11.5 (3″)				
3″	3.469 ddd	9.0 (4″)		78.2 d	141.7	$J_{C\text{-}3'',1''\text{-}H}$=6.2
3″-OCH$_3$	3.408 s			56.4 q		
4″	3.150 ddt	9.3 (5″)		75.9 d	136.7	
5″	3.755 dq (d)	6.25 (6″)		68.1 d		$J_{C\text{-}5'',1''\text{-}H}$=7.6
6″	1.262 d			17.7 q		

Fig. 1. ^{13}C-Relaxation times (seconds) of avermectin B$_{1a}$ in $CDCl_3$ solution at 75.3 MHz and room temperature.

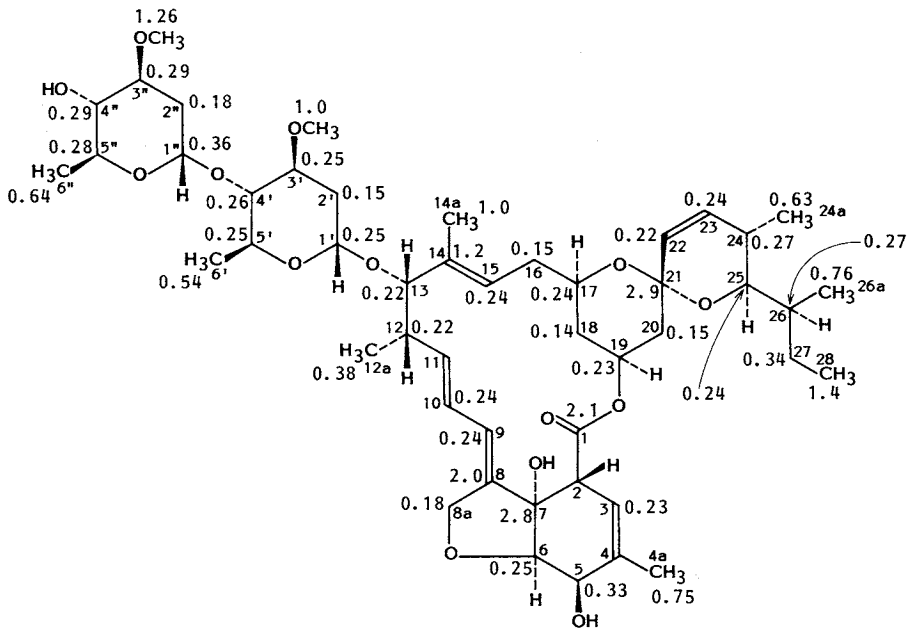

^{1}H NMR parameters in the aglycon of avermectin B$_{1a}$ are consistent with the values found for avermectin A$_{2a}$[6] except for positions 21~24, where the structures differ.

Analysis of the $^3J_{HH}$ spin-spin coupling constants and the values of the anomeric $^1J_{CH}$ constants proved the monosaccharide subunits to be in $^4C_1$ conformation.

All OH protons resonances were observed in the spectrum (broad, chemical shifts values at 4.05 ppm and towards higher field).

In order to study the dynamics of avermectin B_{1a} in solution, ^{13}C NMR relaxation data (T_1) were determined. Experimental T_1 values are shown in Fig. 1.

In the macrocycle there is a nearly uniform distribution of relaxation times of monoprotonated carbon atoms (average $T_1 = 0.23$ s, the rotational correlation time, τ_c is 2.4×10^{-10} seconds if calculated for isotropic reorientation[7]). The isobutyl side-chain shows longer relaxation times, indicative of greater mobility. The disaccharide has additional motional degrees of freedom. The relaxation gradient[8] points from the macrocycle towards the outer oleandrose moiety (the inner monosaccharide shows longer T_1 values than the macrocycle and the outer saccharide has about 20% longer T_1 values than the inner oleandrose).

Conformational energy contour maps were calculated for both glycosidic linkages as functions of the dihedral angles (in steps of 2.5°, see Figs. 2, 3 and Table 3 where the angles are specified). The conformational energy was calculated by conformational analysis of oligosaccharides (CAOS), a molecular modeling program including the HSEA approach[2] in an extended form[9]. There exists, in addition to the global minimum M_0, one local minimum on each map. M_1, the local minimum in the macrocycle–inner oleandrose relation lies about 2.5 kcal·mol^{-1} higher, and M_2 (between the two oleandroses) 4 kcal higher,

Fig. 2. Calculated (HSEA) conformational energy map of the aglycon-oleandrose linkage.

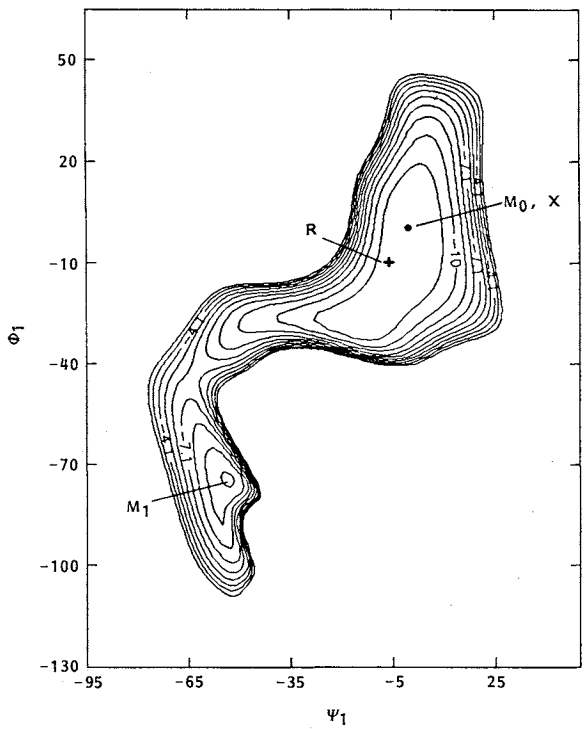

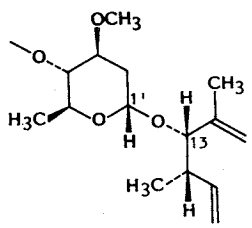

The deepest ten contour levels are drawn with steps of 1 kcal around the global minimum M_0, from where also the relative dihedral angles are measured (degree). M_1 lies higher than M_0 by 2.5 kcal. The crystal conformation X, is close to M_0. R is the NOE restrained minimum, *i.e.* the conformation where all "NOE-distance" restrictions are fulfilled. Table 3 contains the locations of M_0, X and R on the absolute scale.

Fig. 3. Conformational energy map of the oleandrose-oleandrose linkage.

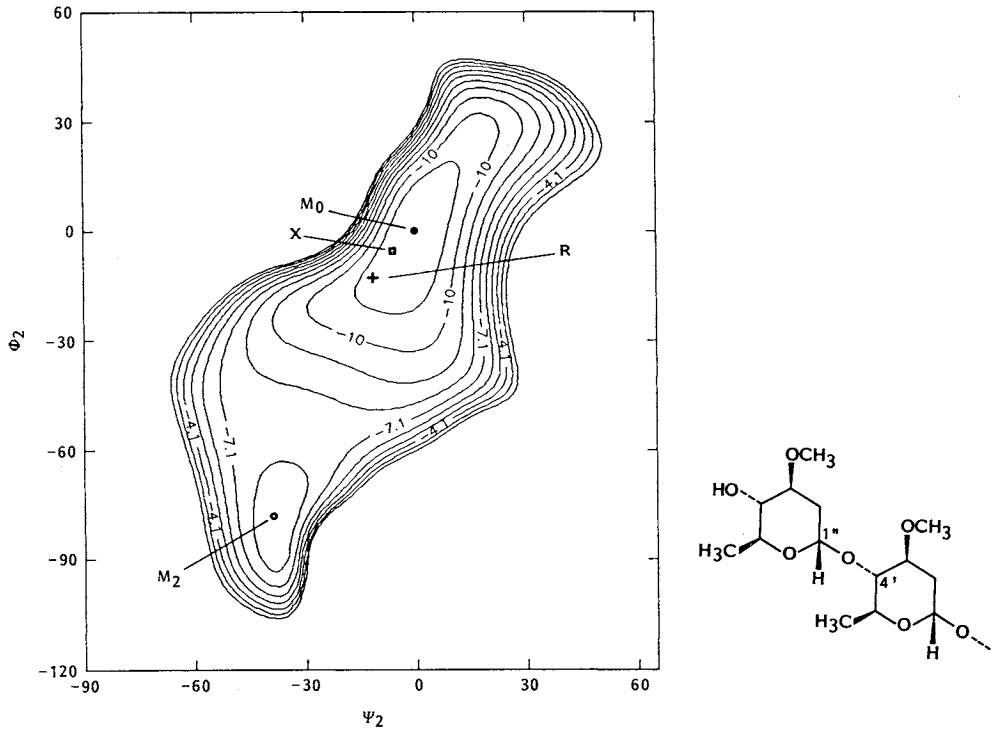

Local minimum M_2 is higher than M_0 by 4 kcal. See also the caption of Fig. 2.

in conformational energy than M_0. Despite the existence of a local minimum, the relative conformation is well defined[10] because the statistical population of the higher energy conformation (M_1 or M_2) should be negligible.

The conformation resulting from the HSEA calculation has been refined by considering the results from nuclear Overhauser enhancement (NOE) experiments. Extensive NOE-difference studies at $\Omega_0 = 400$ MHz, where the value of $\Omega_0\tau_c$ (0.6) is still not unfavorable for the macrocycle (and even better for the saccharides), led to the observation of 12 inter-proton NOE's (of which 7 are inter-residue NOE contacts, shown in Table 2 and on Fig. 4). All NOEs are positive and correspond to interactions between protons ≤ 3.6 Å apart in the refined structure.

"NOE-distances" were generated from relative NOE values using known intra-residue proton-proton distances as a reference (1'-H to 2'-H and 1"-H to 2"-H were chosen). Their error is the same

Table 2. Inter-residue NOE contacts used in structure refinement.

Proton-pair	Distance (Å), structure R[a]	NOE (%) (obscured[b])	NOE (%) (calcd[c])
1' -13	2.67	2.8	3.0
1' -15	2.52	3.3	3.8
5' -12a	2.50	3.5	3.3
1" -4'	2.27	6.9	7.4
5" -4'	3.49	0.9	0.8
5" -6'	2.50	3.5	3.4
28 -16_{eq}	2.90	2.1	2.4

[a] NOE restrained HSEA calculation.

[b] At 400 MHz, the relative error is $< 10\%$. Irradiation sites: 1"-H, 3"-H, 5"-H; 1'-H, 4'-H; 12-H, 12a-H, 13-H, 14a-H and 28-H.

[c] Steady-state NOE fractional enhancements ($f_d(s)$) were calculated from the coupled equations of NOGGLE and SCHIRMER[19] using $\tau_c = 2.4 \times 10^{-10}$ seconds (see text).

Fig. 4. Side view of the solution conformation R of avermectin B_{1a}.

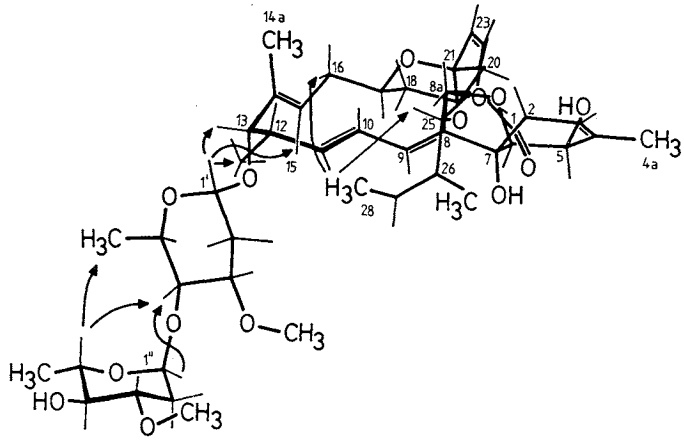

The planes of the macrocycle and the outer oleandrose are both approximately perpendicular to the plane of the inner oleandrose ring. Inter-residue NOE contacts are also shown.

Table 3. Comparison of glycosidic dihedral angles obtained[a] from vicinal spin-spin coupling constants ($^3J_{COCH}$) to dihedral angles of the X-ray structure[12] and of the calculated conformations.

Glycosidic dihedral angle	Dihedral angle (degree)				$^3J_{COCH}$
	X-ray X	HSEA M_0	NOE+HSEA[b] R	Calcd[a] C	expt[c] (Hz)
(1″-H-C-1″-O-C-4′)	41.2	47	35	35<-	3.7
(4′-H-C-4′-O-C-1″)	20.1	30	18	12<-	5.2
(1′-H-C-1′-O-C-13)	50.8	51	41	42<-	3.1
(13-H-C-13-O-C-1′)	37.4	38	31	30<-	4.1

[a] Calculated with MULLOY's constants[13] in the Karplus function.
[b] NOE restrained HSEA calculation. Errors of dihedral angles do not exceed 5°.
[c] Present work (see Experimental part).

as for the NOE observation (*ca.* 10%) because these distances vary only slightly with the solution conformation[5].

Refinement of the HSEA structure was performed by an additional minimization using mild penalty functions[11] for observed NOE contacts.

Glycosidic dihedral angles of the minimum energy HSEA conformations (without and with NOE constraints), and of the X-ray structure[12] are listed in Table 3 together with values calculated from the respective experimental $^3J_{COCH}$ coupling constants (also shown). In order to obtain dihedral angles from the coupling constants a recently reparametrized Karplus-type function was used[13] resulting in the angles in column C.

The conformation calculated by the NOE restrained HSEA energy minimization is corroborated by the four observed $^3J_{COCH}$ coupling constants belonging to the glycosidic linkages: The dihedral angles derived from their values are very close to the dihedral angles characterizing this conformation (columns R and C in Table 3). Therefore the average solution conformation of avermectin B_{1a} seems to be well approximated by conformation R. Of course, the disaccharide can not be regarded as a rigid side chain:

The T_1 gradient reveals the presence of increasing motional freedom. However, this effect may have its origin mainly in the libration along the glycosidic linkages (within potential wells represented on the contour maps of Figs. 2 and 3).

The average solution conformation of avermectin B_{1a} appears to be similar to that found[12] in the crystalline state. The macrocycle is flat and the first oleandrose ring is approximately perpendicular to its plane. The outer oleandrose is nearly parallel to the macrocycle (see Fig. 4 for a side view). This is, however, only qualitatively true. The disaccharide conformation is different in the glycosidic dihedral angles of both linkages of the saccharides (see columns X and R of Table 3).

Intramolecular hydrogen bonds were not observed in solution structure. The conformation is governed mainly through non-bonded interactions. The extensive hydrogen-bonding network found in the X-ray study fixes the avermectin B_{1a} molecules in the crystal lattice and has probably only a minor effect on the disaccharide conformation.

Experimental

NMR Studies

^1H NMR spectra were measured at 600 and 400 MHz, using Bruker AM-600 and Varian XL-400 spectrometers. ^{13}C NMR spectra were taken at 100 MHz. All measurements were performed at 27°C and in $CDCl_3$ with TMS as internal reference. The concentration was 10 mg/0.5 ml for ^1H studies (and 5 times higher for ^{13}C). Correlation spectroscopy (COSY)-45 and NOE spectroscopy (NOESY) maps were recorded at 400 MHz and the ^1H-^{13}C correlation was determined with proton decoupling at 400/100 MHz using standard pulse sequences of the Varian Advance NMR Data System (COSY, NOE2D, HETCOR).

^1H multiplets were analyzed by spin-simulation: The LAOCN3 program (QCPE 111) was revised and modified by the authors to calculate spectra of up to 10 strongly coupled spin 1/2 nuclei on a DEC MicroVAX-II computer.

NOEs were observed in the NOESY spectrum (with a mixing time of 0.6 second) and measured quantitatively with one-dimensional NOE-difference experiments at 400 MHz using decoupler frequency cycling[14] (50 mseconds each, pre-saturation time 5 seconds).

^{13}C NMR T_1 relaxation times were determined at 75 MHz and 30°C (Bruker WM-300) by the inversion-recovery method[15] using composite pulses[16]. The data were analyzed by a three-parameter fit[17]. The statistical error of T_1 values is less than 4%.

$^1J_{CH}$ coupling constants were determined from the proton coupled carbon spectrum.

Inter-subunit $^3J_{CH}$ coupling constants were measured with a precision of 0.2 Hz at 400/100 MHz and 60°C. JIPPO's selective 2D-INEPT method[18] was used, irradiating (10 mseconds, field: 50 Hz) the resonances of 1″-H, 1′-H, 13-H and 4′-H (at 5.41, 4.77, 3.95 and 3.25 ppm) in four experiments. 16 t_1 increments of 256 scans were recorded with sweep widths of 14 Hz in the F1 dimension and 4,096 Hz in the F2 dimension. The digital resolution was 0.11 and 2 Hz, respectively.

Modeling and NOE Restraints

For conformational energy calculation atomic coordinates were taken from crystallographic data[12] (except for C-H distances, which were set to 1.1 Å). The HSEA[2] method was used in an extended form: All hydrogen atoms and hydroxyl groups were included. For methyl and hydroxymethyl hydrogen atoms free rotation was assumed (based on methyl ^{13}C-T_1 data, see Fig. 1).

All calculations were performed with Program CAOS: An interactive, comprehensive molecular-modeling system oriented to organic molecules consisting of several rigid subunits connected through saturated bonds. CAOS has been developed by the authors[9].

Van der Waals interaction is calculated using the HSEA pair-potential between all pairs of atoms within different subunits. Global optimization of all parameters is achieved by stepwise iteration.

Effective NOE potentials (penalty functions) were introduced in some HSEA calculations as restraints. They are represented by attracting harmonic functions, parametrized so that the contribution of each

NOE contact is 2 kcal when its relative error is 10% (following the method of CLORE *et al.*[11]).

The program CAOS also performs T_1 and NOE calculations and is able to estimate various types of ^3J coupling constants. Color graphics representation is provided *via* the program MOLDIS[9] interfaced to CAOS. A DEC MicroVAX-II with a Tektronix 4107A graphics terminal was used for computation and modeling.

Acknowledgments

The authors are indebted to Dr. MICHAEL H. FISHER, Merck Sharp & Dohme Research Laboratories, Rahway, N. J., U.S.A. for a sample of avermectin B_{1a} and the permission to publish these results. We thank Dr. PETER DVORTSAK for taking the 600 MHz NMR spectra (Bruker Application Laboratory, Rheinstetten, Germany).

References

1) THOGERSEN, H.; R. U. LEMIEUX, K. BOCK & B. MEYER: Further justification for the exo-anomeric effect. Conformational analysis based on nuclear magnetic resonance spectroscopy of oligosaccharides. Can. J. Chem. 60: 44~57, 1982
2) BOCK, K.: The preferred conformation of oligosaccharides in solution inferred from high resolution NMR data and Hard Sphere Exo-Anomeric calculations. Pure & Appl. Chem. 55: 605~622, 1983
3) BUSH, C.A.; Z.-Y. YAN & B. N. N. RAO: Conformational energy calculations and proton nuclear Overhauser enhancements reveal a unique conformation for blood group A oligosaccharides. J. Am. Chem. Soc. 108: 6168~6173, 1986
4) BOCK, K.; T. FREJD, J. KIHLBERG & G. MAGNUSSON: Synthetic receptor analogues: the conformation of methyl 4-α-D-galactopyranosyl-β-D-galactopyranoside (methyl β-D-galabioside) and related derivatives, determined by N.M.R. and computational methods. Carbohydr. Res. 176: 253~270, 1988
5) PAULSEN, H.; T. PETERS, V. SINNWELL & B. MEYER: Konformationsanalyse modifizierter Tetrasaccharidsequenzen vom Typ der *N*-Glycoproteine-zum Problem der α-(1->6)-Glycosidischen Bindung. Carbohydr. Res. 165: 251~266, 1987
6) ALBERS-SCHÖNBERG, G.; B. H. ARISON, J. C. CHABALA, A. W. DOUGLAS, P. ESKOLA, M. H. FISHER, A. LUSI, H. MROZIK, J. L. SMITH & R. L. TOLMAN: Avermectins. Structure determination. J. Am. Chem. Soc. 103: 4216~4221, 1981
7) WEHRLI, F. W.: Organic structure assignments using ^{13}C spin-relaxation data. *In* Topics in Carbon-13 NMR Spectroscopy. Vol. II. *Ed.*, G. C. LEVY, p. 350, Wiley, 1976
8) NESZMÉLYI, A.; A. LIPTÁK, P. NÁNÁSI & J. SZEJTLI: C-13 relaxation time gradients in complexes of linear oligosaccharides and cyclodextrin. Acta Chim. Hung. 113: 431~436, 1983
9) NESZMÉLYI, A. & J. HOLLÓ: Some aspects of the structure of starch—a 3-D molecular modelling approach. J. Mol. Graphics, in press
10) CUMMING, D. A. & J. P. CARVER: Virtual and solution conformation of oligosaccharides. Biochemistry 26: 6664~6676, 1987
11) CLORE, G. M.; A. M. GRONENBORN, A. T. BRÜNGER & M. KARPLUS: Solution conformation of a heptadecapeptide. J. Mol. Biol. 186: 435~455, 1985
12) SPRINGER, J. P.; B. H. ARISON, J. M. HIRSHFIELD & K. HOOGSTEEN: The absolute stereochemistry and conformation of avermectin B_{2a} aglycon and avermectin B_{1a}. J. Am. Chem. Soc. 103: 4221~4224, 1981
13) MULLOY, B.; TH. A. FRENKIEL & D. B. DAVIES: Long-range carbon-proton coupling constants: Application to conformational studies of oligosaccharides. Carbohydr. Res. 184: 39~46, 1988
14) KINNS, M. & J. K. M. SANDERS: Improved frequency selectivity in nuclear Overhaueser effect difference spectroscopy. J. Magn. Reson. 56: 518~520, 1984
15) VOLD, R. E.; J. S. WAUGH, M. P. KLEIN & D. E. PHELPS: Measurement of spin relaxation in complex systems. J. Chem. Phys. 48: 3831~3832, 1968
16) LEVITT, M. H. & R. FREEMAN: NMR population inversion using a composite pulse. J. Magn. Reson. 33: 473~476, 1979
17) SASS, M. & D. ZIESSOW: Error analysis for optimized inversion recovery spin-lattice relaxation measurement. J. Magn. Reson. 25: 263~278, 1977
18) JIPPO, T.; O. KAMO & K. NAGAYAMA: Determination of long-range proton-carbon 13 coupling constants with selective two-dimensional INEPT. J. Magn. Reson. 66: 344~348, 1986
19) NOGGLE, J. H. & R. E. SCHIRMER: The Nuclear Overhauser Effect. Academic Press, 1971